

# Comparative LIDT measurements of optical components for high-energy HiLASE lasers

Jan Vanda<sup>1</sup>, Jan Ševčík<sup>1</sup>, Egidijus Pupka<sup>2</sup>, Mindaugas Ščiuka<sup>2</sup>, Andrius Melninkaitis<sup>3</sup>, Martin Divoký<sup>1</sup>, Venkatesan Jambunathan<sup>1</sup>, Stefano Bonora<sup>1,4</sup>, Václav Škoda<sup>5</sup>, Antonio Lucianetti<sup>1</sup>, Danijela Rostohar<sup>1</sup>, Tomas Mocek<sup>1</sup>, and Valdas Sirutkaitis<sup>3</sup>

<sup>1</sup>Hilase, Institute of Physics AS CR, Za Radnicí 828, 252 41 Dolní Břežany, Czech Republic

<sup>2</sup>LIDARIS Ltd., Saulėtekio Al. 10, LT-10223, Vilnius, Lithuania

<sup>3</sup>Laser Research Center, Vilnius University, Sauletekio Al. 10, LT-10223 Vilnius, Lithuania

<sup>4</sup>LUXOR Laboratory, CNR IFN, Via Trasea 7, 35131, Padova, Italy

<sup>5</sup>Crytur Ltd., Palackeho 175, 511 01 Turnov, Czech Republic

(Received 23 December 2015; revised 2 February 2016; accepted 23 February 2016)

## Abstract

Further advancement of high-energy pulsed lasers requires a parallel development of appropriate optical components. Several different optical components, such as mirrors and antireflection-coated windows, which are essential for the design of HiLASE high average power lasers were tested. The following paper summarizes results on the measurements of laser-induced damage threshold of such components, and clearly shows their capabilities and limitations for such a demanding application.

**Keywords:** diode-pumped solid-state laser and applications; laser-induced damage

## 1. Introduction

The laser-induced damage threshold (LIDT) is the highest quantity of laser radiation incident upon the optical component for which the extrapolated probability of damage is zero<sup>[1]</sup>. As a consequence, it is easy to understand why the LIDT is a key parameter for all optical components which will be used in design of any high-power laser systems. The importance of the LIDT of each optical component in such type of laser systems is reflected by the fact that the LIDT establishes the limits of maximum achievable energy of a whole laser system. Reliable and stable laser sources, desirable for both the academic and the industrial sector, require a careful testing and a development of involved optical components to meet certain quality criteria. In addition, the LIDT is also a limiting factor for the laser beam distribution system (LBDS), a system of optical components used to deliver such powerful laser pulses toward an area of scientific and industrial application.

Although the LIDT testing is a part of common procedures conducted by optical component manufacturers, the components are not tested for these extreme radiation conditions

provided by newly developed lasers. At HiLASE center the development of scalable kW-class diode-pumped solid-state pulsed lasers is taking place. In order to support both the laser system development and design of the LBDS, both stock components and prototyped parts developed at HiLASE center have been tested in a facility accessible in Vilnius through the LaserLab Europe initiative.

A number of different components were tested for the LIDT in multipulse regime (s-on-1), where the most important were mirrors and antireflection-coated (AR) windows. Components were tested under laser radiation conditions according to their intended use at ps and ns pulse lengths for 10<sup>3</sup> (ns case) and 10<sup>5</sup> (ps case) pulses. ISO 21254 standards series compliance of the testing facility further ensures the reliability and the validity of the obtained results.

Tested components were provided both by commercial companies as their standard optical components as well as by various manufacturers as customized optics. Obtained LIDT values were very scattered and similar parts from different vendors demonstrated significant differences in damage threshold. All results will be used to identify respective components suitable for the HiLASE laser systems as well as for the further development of the LBDS.

Correspondence to: J. Vanda, Hilase, Institute of Physics AS CR, Za Radnicí 828, 252 41 Dolní Břežany, Czech Republic. Email: [vandaj@fzu.cz](mailto:vandaj@fzu.cz)

**Table 1.** Conditions for testing with nanosecond pulses.

Pulse length	Maximal pulses per site	Polarization state	Repetition rate	Spot beam diameter ( $1/e^2$ , $0^\circ$ AOI)	Environment
10 ns	$10^3$	P	10 Hz	0.245 mm	Ambient air

## 2. Motivation

There are several laser systems within the HiLASE center with different demands regarding the LIDT of used components<sup>[2, 3]</sup>.

According to the intended use, all tested samples can be divided in two main testing batches—regime with pulse duration of 1 ps and 1 kHz repetition rate and regime with pulse duration 10 ns and 10 Hz repetition rate. This distribution also corresponds with the testing facility capabilities, where ps and ns measurements were realized at different setups. The goal of measurements is to evaluate and approve the components from certain manufacturers for use in respective laser systems (beamlines A–C and multislab). All samples, before testing, were cleaned with respect to the manufacturer recommendations in a clean environment (ISO class 7) by air blowing and drop and drag wiping technique using ethanol (99.7%) and lens tissues. The samples were then packed into dust-free optic storage boxes and kept sealed until testing.

### 2.1. Samples irradiated by ns pulses (multislab system)

Fifteen different optical components were prepared for the LIDT tests, representing parts required for the multislab laser system realization. In particular, samples included high reflective (HR) dielectric mirrors, AR-coated windows, thin film polarizers and dichroic beam splitters. Coatings and deposition methods were not specified, as the purpose of prepared tests is to show the performance of particular samples. In this paper, only LIDT measurements on HR dielectric mirrors and AR-coated windows will be discussed. These two types of samples are sufficient to demonstrate importance of the LIDT testing and to show the most important results. The test conditions summarized in Table 1 were selected considering assumed accumulated radiation of components in the laser system.

The list of tested components specifying its type, dimensions and angle of incidence (AOI) is summarized in Table 2.

### 2.2. Samples irradiated by ps pulses (beamlines A–C)

Nine different optical components were prepared for the LIDT tests, and selected from metallic mirrors, hybrid mirrors and experimental dielectric AR coatings. Similar to the previous case, only LIDT measurements on metallic and

**Table 2.** List of components tested at ns regime.

Sample no.	Type	Size/shape	AOI (deg.)
09	HR mirror	1"/round	45
10	AR window	1"/round	0
13	AR window	1"/round	0
14	AR window	1"/round	0
15	AR window	1"/round	0
16	AR window	1"/round	0
18	AR window	25 mm/round	0
22	HR mirror	40 mm/square	0

**Table 3.** Conditions for testing with picosecond pulses.

Pulse length	Pulses per site	Polarization state	Repetition rate	Spot beam diameter ( $0^\circ$ )	Environment
1 ps	$10^5$	P	1 kHz	0.042 mm	Ambient air

**Table 4.** List of components tested at ps regime.

Sample no.	Type	Size/shape	AOI (deg.)
01	Hybrid mirror	1"/round	45
02	Hybrid mirror	1"/round	45
03	Hybrid mirror	1"/round	45
05	Protected silver mirror	1"/round	45
07	Protected gold mirror	1"/round	45

hybrid mirrors will be discussed further. Coatings and deposition methods were not specified, as the purpose of prepared tests is to show the performance of particular samples.

Broadband mirrors (metallic and hybrid) are important for the future use of picosecond laser systems (see Figure 1). While the output of these lasers is intended for the wavelength tuning to NIR, broadband mirrors will be required to deliver both fundamental wavelength and tuned output in the range 1.6–4  $\mu\text{m}$  toward application laboratories using a single beam delivery path<sup>[4, 5]</sup>.

The following test conditions (see Table 3) were selected considering assumed accumulated radiation of components in the laser system.

In Table 4 is the list of tested components specifying its type, dimensions and AOI.

### 2.3. Testing facility

The LIDT testing facility was kindly provided by the Vilnius University that was operated in cooperation with the company LIDARIS Ltd. The facility has well-settled testing stations according to ISO 21254 standard series recommendations (block scheme on Figure 2) and it is able to produce ISO 21254 compliant test reports<sup>[6]</sup>.

The LIDT setup design follows the ISO recommendations both for the beam delivery and the specimen part. The LIDT measurement is fully automated, which significantly speeds up the testing process. Online damage detection is based on the detection of the scattered light, following ISO

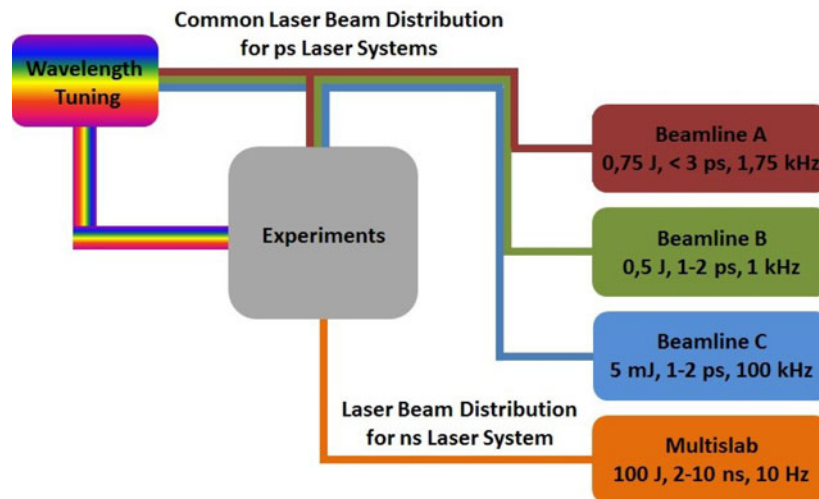


Figure 1. Schematics of laser systems developed at HiLASE project and respective LBDSs.

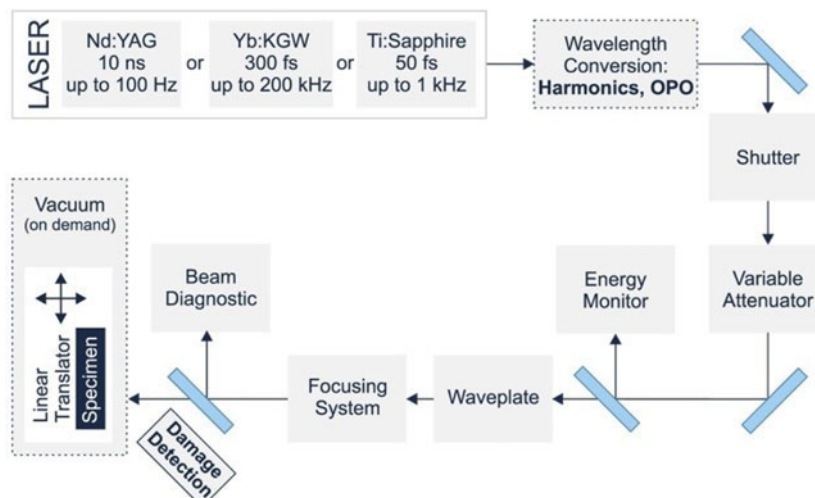


Figure 2. Block scheme of the LIDT testing setup at LIDARIS.

standard recommendations as well. The facility is equipped with a Nomarski type microscope for the optical inspection of specimens after the exposure, to check the data from the online damage detection. Overall, the facility allows reliable and reproducible LIDT testing of optical components for conditions under which tested optics is intended to be used.

### 3. Measurement and evaluation

#### 3.1. Test conditions

A Nd:YAG laser provided pulses with duration of 10 ns and repetition rate of 10 Hz for the LIDT test. The emission wavelength of the laser was 1064 nm while tested samples were mentioned for use at 1030 nm. However, respective spectra of samples were known from manufacturers and all

spans over 1064 nm. The spot diameter was set up at 0.245 mm at normal incidence ( $1/e^2$ ), which allows more than 300 test sites on the surface of 1" or 25 mm diameter components. In order to prevent influence of one site to other, a site diameter was set to 1 mm. For technical reasons, the active area for all components was set up round, with 20 mm in the diameter except for 40 mm square samples, where the active area was set up round, 32 mm in the diameter.

An Yb:KGW laser with stretched pulse length 1 ps and repetition rate 1 kHz was the source for LIDT tests under ps pulses. The emission wavelength of the Yb:KGW system was 1030 nm. The spot diameter was set up at 0.048 mm at normal incidence, which allows over 2000 test sites on the surface of 1" or 25 mm diameter components. In this set of testing, the site diameter was set to 0.28 mm. The

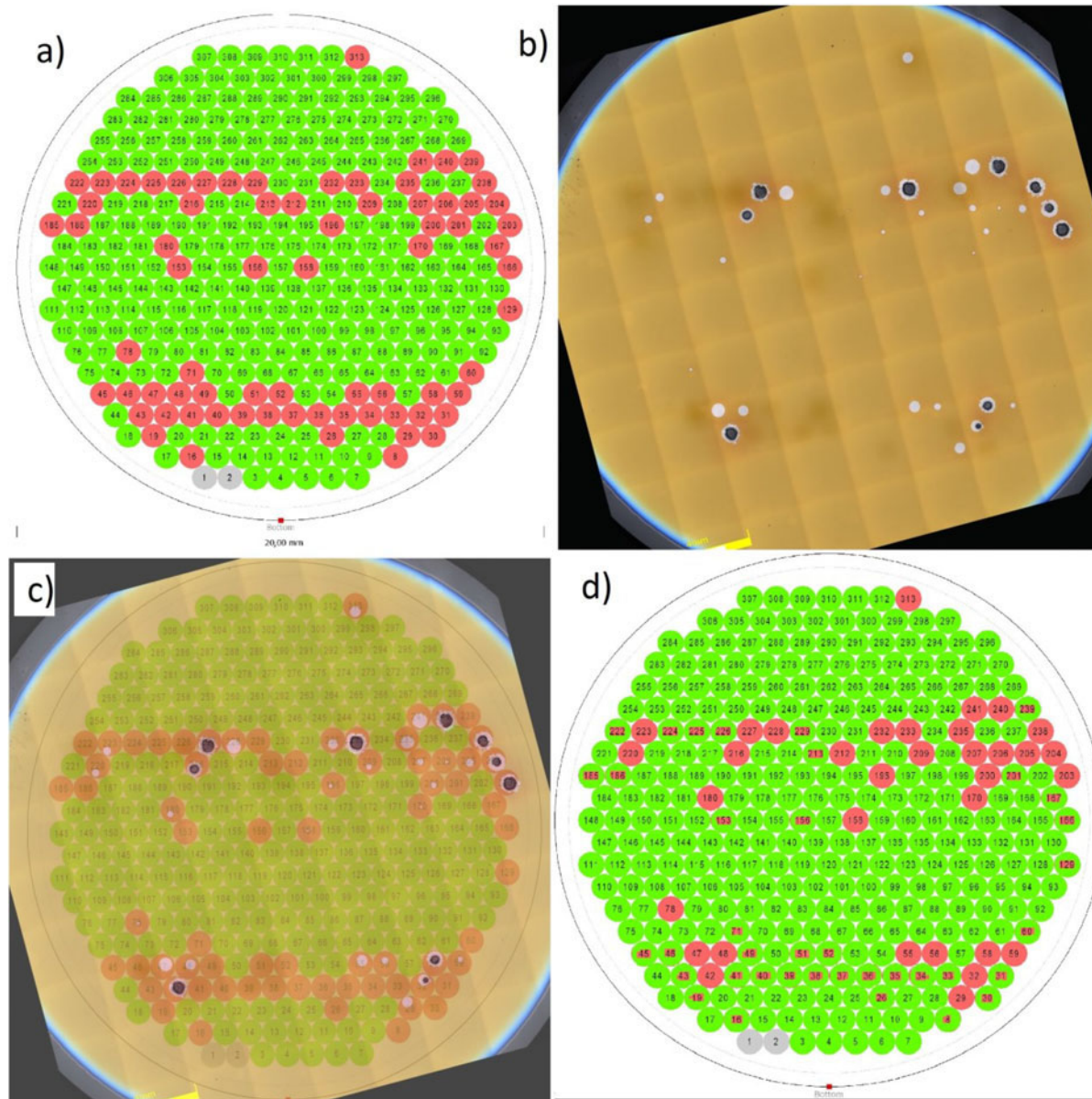


**Figure 3.** Mirror surface; (a) map of exposure sites, red are noted as damaged according to the scattering light detection; (b) surface of damaged sample by Nomarski microscopy; (c) the sample surface superimposed with the map; (d) the corrected map of sites after the optical inspection.

active area for all samples was the same as for the case of ns samples, i.e., it was round with a diameter of 20 mm. In this case, the spot size does not agree with the ISO 21254 recommendations, which suggests that the size of laser spots should not be smaller than 0.2 mm in the target plane. This fact has to be taken into account during later evaluation of the test results.

### 3.2. Test procedure

All samples were mounted on a frame which was fixed at a XY motorized stage. The whole process of testing, including

the positioning of the sample, the laser beam monitoring and the damage detection was software controlled. In a first step, the active area was divided according to the spot diameter to sites (as it can be seen in Figure 3(a)). Then, the sites were exposed to trains of laser pulses (number of pulses in the train according to Tables 1 and 3) with constant pulse energy. In the first couple of dozens sites the pulse energy is changed for every site to gather information about the approximate laser pulse energy which will induce damage. The next step is to set according to gathered results a likely highest safe pulse energy, which will not induce any damage, and expose ten sites. If no damage is detected at those ten sites, the energy is increased and another ten sites are exposed. This

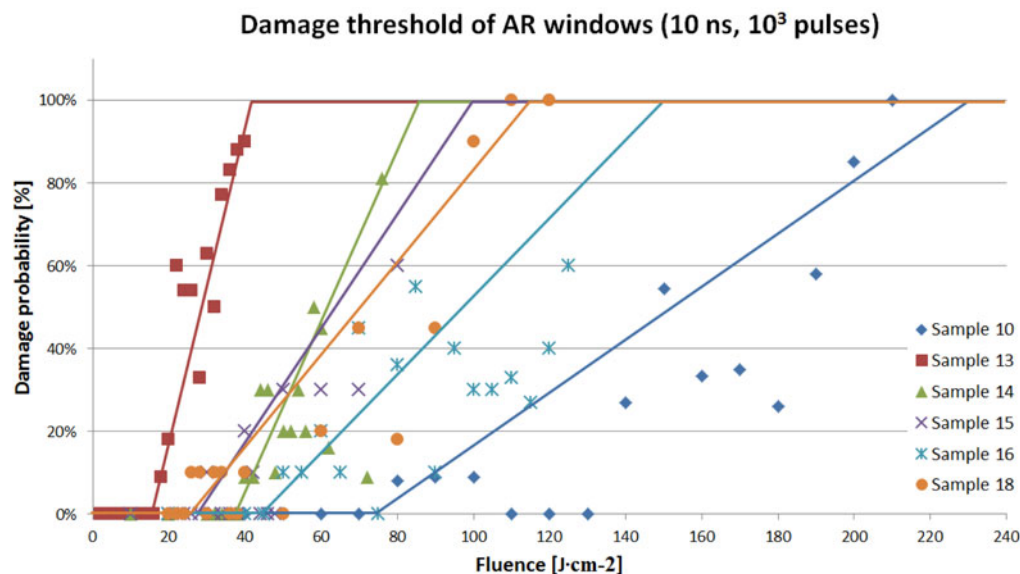


**Figure 4.** Damage threshold curves for AR-coated windows tested with ns pulses.

procedure is done until the pulse energy at which all ten sites are damaged is found or there are no unexposed left sites. This procedure goes similarly for both ns and ps systems. In ps system case, significantly larger number of sites allows much smaller steps in increasing energy of the pulses, so damage threshold can be defined more precisely. During the exposure, the scattered light detection realized with a photodiode was used as online damage detection. Once the detected scattered light intensity was on the previously defined level of intensity corresponding to scattered light from a damaged site, the control software interrupted the exposure, marked the respective site as damaged, moved to the next site and continued in the procedure. In the other case, when the detected intensity of the scattered light does not reach a pre-defined level, the software will take care that an exact number of laser pulses are delivered for each site (see Tables 1 and 3).

### 3.3. Data collection

When the testing procedure was finished, samples were observed by a Nomarski type microscope in order to check all sites. This step is necessary due to the inaccuracy of the damage detection based on a scattered light. The detection system can be, for example, confused by detecting the light scattered from dust particles in air or by detecting a reflected light from highly reflective samples under high pulse energies and detects false damage. Similarly, in the case of highly transparent samples, the damage detection system can miss the damage event because of a low scattered light intensity. Also, interference coming from the environment can affect the damage detection. In order to correct possible errors in detection of damaged sites, the images of the sample

**Table 5.** Damage thresholds of AR-coated windows; linearly extrapolated values were rounded down to closest integer.

Sample	Damage threshold ( $\text{J cm}^{-2}$ )
10	73
13	17
14	38
15	28
16	45
18	23

surface where damaged sites are recognized (Figure 3(b)) are compared with a map of exposed sites (Figure 3(c)). The optical analysis allowed correction of false damaged sites or missed sites. As a result, the final exposure map for further analysis was produced (Figure 3(d)). The pulse energies applied to each specific site were saved during the test procedure and exported into an excel table.

## 4. Results and discussion

### 4.1. Damage threshold of samples tested at 10 ns pulse length

Tables 5 and 6 summarize the damage threshold value estimated using above described procedure, Figures 4 and 6 shows damage threshold curves extrapolated according to the ISO 21254-2 recommendations. Information about the site number, the damage status, the number of pulses and the fluence calculated from the corresponding laser intensity and the spot diameter, needed for calculations, were extracted from excel tables, generated for the each sample. Such data were further analyzed to obtain respective damage probabil-

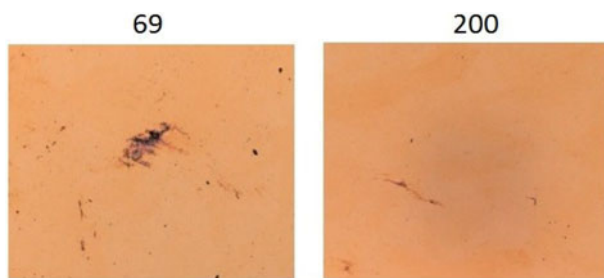


**Figure 5.** Microscope images of sample 15 sites 69 and 200, marked as damaged, with notable scratches and dents not caused by laser.

**Table 6.** Damage thresholds of HR dielectric mirrors, linearly extrapolated values were rounded down to the closest integer.

Sample	Damage threshold ( $\text{J cm}^{-2}$ )
09	10
22	93

ity curves for each sample. Probabilities and extrapolation of damage threshold were calculated according to the recommendations of ISO 21254-2 standard<sup>[1]</sup>.

The most interesting samples for multislabs nanosecond laser system at the actual state of the development were windows for vacuum chambers. As can be seen from the resulting table, the damage threshold values were quite scattered: samples with damage threshold below  $20 \text{ J cm}^{-2}$  as well as samples with damage threshold over  $70 \text{ J cm}^{-2}$  were found. The irregular slope of damage probability curve in the case of samples 15 and 18 suggests the existence of surface defects<sup>[7, 8]</sup>, which may affect the LIDT. This

suspicion was confirmed by the inspection of the sample 15 with a laser scanning microscope (Figure 5).

Investigation of the surface of the sample 15 revealed scratches on the area of damaged spots, which most likely decreased the LIDT of this particular sample. Thereafter, particular spots with identified scratches were excluded from the LIDT extrapolation. However, no defects were found on the surfaces of remaining samples, which implies that the damage thresholds of other samples can be related with properties of manufactured coatings and substrates.

The procedure used for calculating the LIDT on AR windows was also used for the HR mirrors. In the development of multislabs laser systems, one of the most critical optical components is the HR mirrors for the deformable mirror. There were two samples tested: the sample 09 was a common mirror from a commercial supplier, while the sample 22 was a prototype of dielectric mirror developed in cooperation with a research partner. Damage threshold difference between these two samples is extremely high (see Table 6) and encourages further efforts in the development of novel adaptive optical mirrors.

#### 4.2. Damage threshold of samples tested at 1 ps pulse length

The same approach as in the case of LIDT measurements at 10 ns long pulses was used for the evaluation of results obtained from the ps testing setup. Results were again saved in excel tables, containing information about the site number, the damage status, the number of pulses and the laser fluence calculated from the laser energy and the spot diameter. Despite the beam diameter not matching ISO 21254 recommendations, probabilities and resulting extrapolation of damage thresholds were calculated according to this

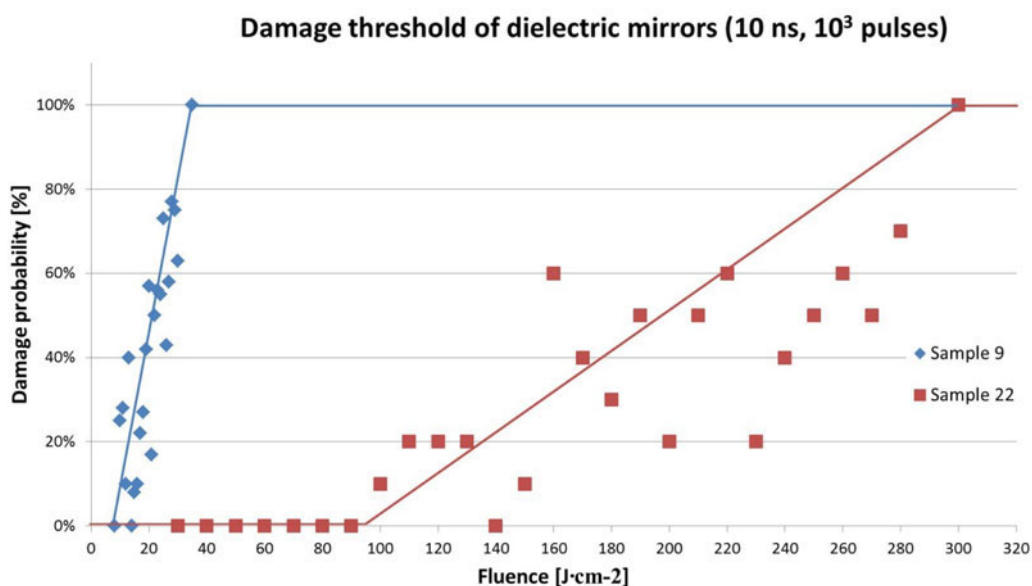


**Figure 6.** Damage threshold curves for HR dielectric mirrors tested with ns pulses.

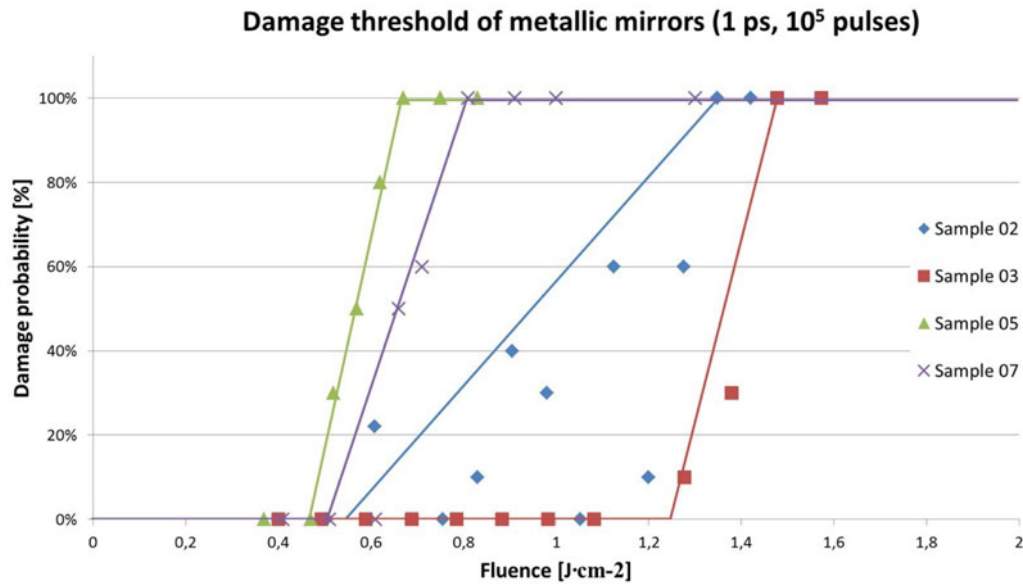


Figure 7. Damage threshold curves for mirrors tested with ps pulses.

Table 7. Damage thresholds of mirrors, linearly extrapolated values were rounded down to two decimals.

Sample	Damage threshold ( $\text{J cm}^{-2}$ )
02	0.55
03	1.25
05	0.47
07	0.51

standard. Common protected metallic mirrors (the samples 05 and 07) can be used as a standard for further development, because their technology is well described and the LIDT is reproducible.

As can be seen from Figure 7 and Table 7, damage thresholds values were scattered from approximately  $0.5 \text{ J cm}^{-2}$  in the case of commercial protected metallic (silver and gold) mirrors up to  $1.25 \text{ J cm}^{-2}$  in the case of experimental hybrid mirror. The surface inspection with laser scanning microscope did not find any explanation for the irregular slope of damage probability in the case of sample 02. It is assumed that the uneven dependence of the LIDT on the fluence is caused by manufacturing process. On the contrary, sample 03, hybrid mirror based on silver, indicated quite high damage threshold despite the detectable silver layer degradation.

#### 4.3. Damage morphology

Damage morphology is an integral part of the laser-induced damage tests, while it can point at damage precursors and causes<sup>[9, 10]</sup>. The ISO 21254-2 standard recommends an inclusion of damage morphology micrographs into the gen-

erated damage threshold reports. Figures 8(a–d) were obtained using a laser scanning microscopy, which allows the detailed study of craters and effective data storage for a future analysis, including full 3D topology information.

The observed craters on all samples of interest represent typical damages of dielectric multilayers on dielectric substrate in the case of multipulse exposure at nanosecond pulse length scale. This type of damage is usually related to the evaporation and the plasma formation, which is linked to the thermally induced damage. Altered region around the crater is caused by redeposition of the high-pressure evaporated material<sup>[9]</sup>.

In the case of metallic and hybrid mirrors one can easily observe some differences in the morphology of the crater. Unlike the nanosecond case, craters caused by the damage from picosecond pulses are more localized, with sharp edges corresponding to the beam diameter—the damage looks more like a hole drilled to the surface (see Figure 9). Using a high magnification, one can observe nanosized debris of the coating around the crater ejected by rapid expansion of the plasma. A 3D topograph reveals typical ‘collar’ of the redeposited material around the crater. Whitish stains observable in Figure 8(b) are, according to the manufacturer, caused by degradation of the silver layer below dielectric layers. It can be attributed to the unstable conditions during the sputtering process and it is not related with the laser exposure of the sample.

## 5. Conclusion

A considerable number of components intended for use in high-energy laser systems within HiLASE center were

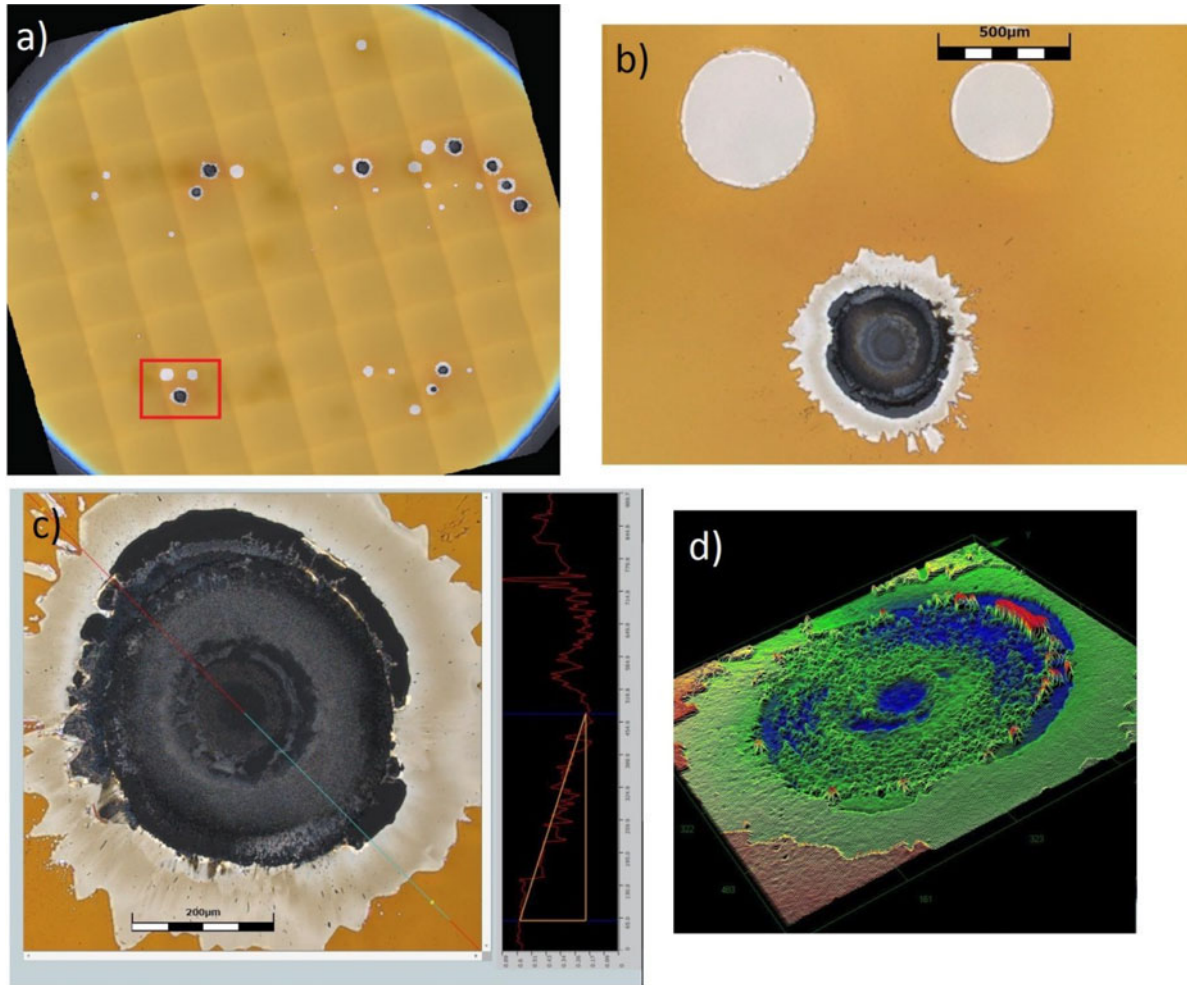


**Figure 8.** Damaged coating of the sample 10 (AR-coated window), where the sample was exposed to ns pulse trains; (a) the marked area of interest, (b) (from upper left) the site 47 (2 pulses at energy  $170 \text{ J cm}^{-2}$ ); the site 48 (4 pulses at energy  $170 \text{ J cm}^{-2}$ ); the site 42 (96 pulses at energy  $170 \text{ J cm}^{-2}$ ); (c) a close look at the site 42; (d) 3D height topology (wire surface) of the site 42.

successfully tested. These optical components were mostly dielectric-coated windows (AR coating) or mirrors (HR on metallic or dielectric substrate). Damage threshold tests were conducted at ISO 21254-series standards compliant station, which ensured the reproducibility and the reliability of obtained results.

In the case of AR-coated windows tested under nanosecond pulses extremely high values of LIDT exceeding  $40 \text{ J cm}^{-2}$  were demonstrated. In this sense, the sample 10 ( $73 \text{ J cm}^{-2}$ ) and the sample 15 ( $45 \text{ J cm}^{-2}$ ) performed very well and will be highly considered for the design of our laser system. In the case of HR dielectric mirrors, the tested prototype (the sample 22) exhibited an outstanding damage threshold exceeding  $93 \text{ J cm}^{-2}$ , which is several times more than the best mirrors available on the market.

A satisfactory performance of components tested under picosecond regime was also observed. Although the technology of producing hybrid mirrors is not well handled yet,

prototypes under investigation demonstrated a significantly better damage threshold than common protected metallic mirrors. Therefore, there is reasoned assumption that such mirrors can be effectively used for broadband LBDSs.

### Acknowledgments

The research leading to these results has received funding from LASERLAB-EUROPE (grant agreement no. 284464, EC's Seventh Framework Programme).

This work is co-financed by the European Regional Development Fund, the European Social Fund and the state budget of the Czech Republic (project HiLASE: CZ.1.05/2.1.00/01.0027, project DPSSLasers: CZ.1.07/2.3.00/20.0143, project Postdok: CZ.1.07/2.3.00/30.0057). This research was partially supported by the grant RVO 68407700.

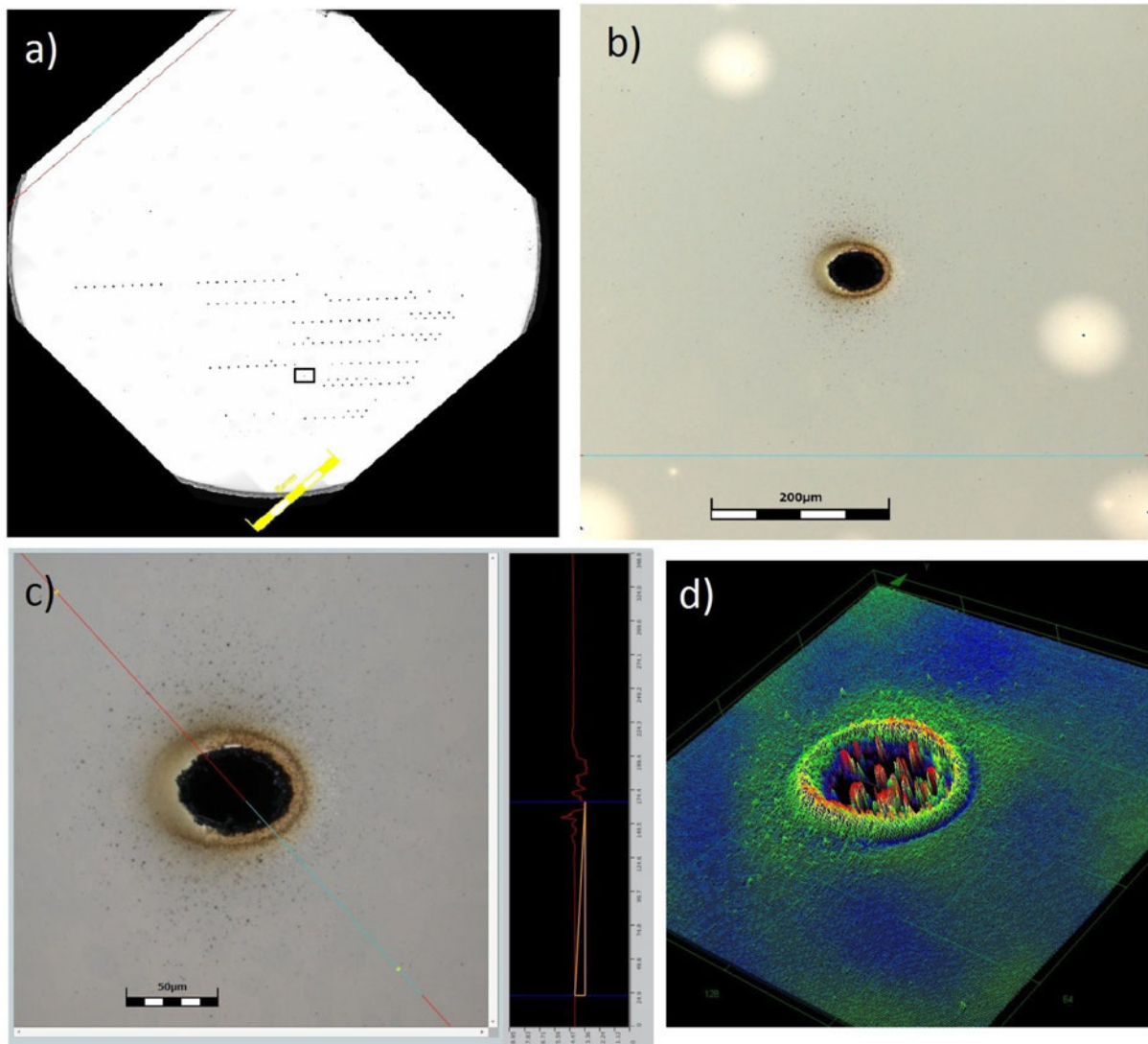


**Figure 9.** Damaged coating of the sample 03 (the hybrid mirror), the sample was exposed to the train of ps pulses; (a) the marked area of interest, (b) the site 276 (407 pulses at the energy  $1.47 \text{ J cm}^{-2}$ ); (c) the close look to the site 276; (d) 3D height topology (wire surface) of the site 276.

## References

1. International Organization for Standardization, ISO 21254-1:2011—Lasers and laser-related equipment—Test methods for laser-induced damage threshold (ISO, Geneva, 2011).
2. M. Divoky, M. Smrz, M. Chyla, P. Sikocinski, P. Severova, O. Novák, J. Huynh, S. S. Nagisetty, T. Miura, C. Liberatore, J. Pilař, O. Slezak, M. Sawicka, V. Jambunathan, L. Gemini, J. Vanda, R. Svabek, A. Endo, A. Lucianetti, D. Rostohar, P. D. Mason, P. J. Phillips, K. Ertel, S. Banerjee, C. Hernandez-Gomez, J. L. Collier, and T. Mocek, *Proc. SPIE* **9255**, 92550V (2015).
3. O. Novák, T. Miura, M. Smrz, M. Chyla, S. S. Nagisetty, J. Mužík, J. Linnemann, H. Turčičová, V. Jambunathan, O. Slezák, M. Sawicka-Chyla, J. Pilař, S. Bonora, M. Divoký, J. Měsíček, A. Pranovich, P. Sikocinski, J. Huynh, P. Severová, P. Navrátil, D. Vojna, L. Horáčková, K. Mann, A. Lucianetti, A. Endo, D. Rostohar, and T. Mocek, *Appl. Sci.* **5**, 637 (2015).
4. B. Wang and L. Gallais, *Opt. Express* **21**, 14698 (2013).
5. J. Vanda, O. Novak, A. Hervy, and V. Skoda, *Proc. SPIE* **9237**, 92371B (2014).
6. A. Melninkaitis, D. Miksys, T. Balciunas, O. Balachninaite, T. Rakickas, R. Grigonis, and V. Sirutkaitis, *Proc. SPIE* **6101**, 61011J (2006).
7. L. Gallais, J. Y. Natoli, and C. Amra, *Opt. Express* **10**, 1465 (2002).
8. H. Krol, L. Gallais, C. Grezes-Besset, D. Torricini, and G. Lagier, *Opt. Eng.* **46**, 023402 (2007).
9. R. M. Wood, *Laser-Induced Damage of Optical Materials* (Institute of Physics Publishing Ltd, Bristol, 2003).
10. H. He, H. Hu, Z. Tang, Z. Fan, and J. Shao, *Appl. Surf. Sci.* **241**, 442 (2005).